This article was downloaded by:
On: *22 January 2011*
Access details: *Access Details: Free Access*
Publisher *Taylor & Francis*
Informa Ltd Registered in England and Wales Registered Number: 1072954 Registered office: Mortimer House, 37-41 Mortimer Street, London W1T 3JH, UK

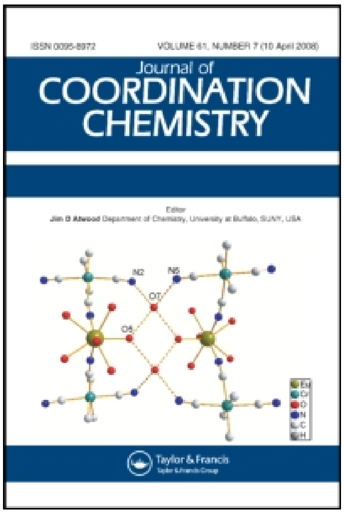

Journal of Coordination Chemistry

Publication details, including instructions for authors and subscription information:
http://www.informaworld.com/smpp/title~content=t713455674

Synthesis, structure, and magnetic behavior of a pyrazine-bridged Cu(II)/Au(CN)$_2$ complex

Sarah J. Ludy[a]; Christopher P. Landee[b]; Mark M. Turnbull[a]; Jan L. Wikaira[c]
[a] Carlson School of Chemistry and Biochemistry, Clark University, Worcester, MA 01610, USA [b] Department of Physics, Clark University, Worcester, MA 01610, USA [c] Chemistry Department, University of Canterbury, Christchurch, 8041, New Zealand

First published on: 22 December 2010

To cite this Article Ludy, Sarah J. , Landee, Christopher P. , Turnbull, Mark M. and Wikaira, Jan L.(2011) 'Synthesis, structure, and magnetic behavior of a pyrazine-bridged Cu(II)/Au(CN)$_2$ complex', Journal of Coordination Chemistry, 64: 1, 134 — 144, First published on: 22 December 2010 (iFirst)

To link to this Article: DOI: 10.1080/00958972.2010.543459

URL: http://dx.doi.org/10.1080/00958972.2010.543459

PLEASE SCROLL DOWN FOR ARTICLE

Full terms and conditions of use: http://www.informaworld.com/terms-and-conditions-of-access.pdf

This article may be used for research, teaching and private study purposes. Any substantial or systematic reproduction, re-distribution, re-selling, loan or sub-licensing, systematic supply or distribution in any form to anyone is expressly forbidden.

The publisher does not give any warranty express or implied or make any representation that the contents will be complete or accurate or up to date. The accuracy of any instructions, formulae and drug doses should be independently verified with primary sources. The publisher shall not be liable for any loss, actions, claims, proceedings, demand or costs or damages whatsoever or howsoever caused arising directly or indirectly in connection with or arising out of the use of this material.

Journal of Coordination Chemistry
Vol. 64, No. 1, 10 January 2011, 134–144

Taylor & Francis
Taylor & Francis Group

Synthesis, structure, and magnetic behavior of a pyrazine-bridged Cu(II)/Au(CN)$_2$ complex

SARAH J. LUDY†, CHRISTOPHER P. LANDEE‡,
MARK M. TURNBULL*† and JAN L. WIKAIRA§

†Carlson School of Chemistry and Biochemistry, Clark University, 950 Main St.,
Worcester, MA 01610, USA
‡Department of Physics, Clark University, 950 Main St., Worcester, MA 01610, USA
§Chemistry Department, University of Canterbury, PB 4800, Christchurch,
8041, New Zealand

(*Received 3 August 2010; in final form 17 November 2010*)

The reaction of $Cu(ClO_4)_2 \cdot 6H_2O$ with pyrazine (pz) and $KAu(CN)_2$ in DMSO generates $[CuAu(CN)_2(pz)(DMSO)_2]Au(CN)_2$ (**1**). Monoclinic, *P2₁/c*: $a = 6.8727(2)$ Å, $b = 10.2230(3)$ Å, $c = 14.1923(4)$ Å, $\beta = 90.0100(10)°$. The complex forms 2-D sheets with Cu(II) bridged parallel to the *a*-axis by pyrazine molecules and parallel to the *b*-axis by one of the dicyanoaurates (containing Au1). The copper coordination sphere is completed with two O-coordinated DMSO molecules which exhibit short S–Au contacts to Au1 in the adjacent layers. A crystallographically independent $Au(CN)_2^-$ ion (containing Au2) provides charge balance and is held in the lattice *via* Au–Au contacts (Au1–Au2 = 3.436(4) Å). The complex exhibits vapochromic properties. Although stable in dry air at room temperature, green crystals of **1** subjected to a water atmosphere turn pale blue as the DMSO molecules are lost. Other vapors (NH_3, $PrNH_2$, py, etc.) generate solvates with a wide variety of colors.

Keywords: Magnetism; X-ray structure, Coordination chemistry; Cu(II); Dicyanoaurate

1. Introduction

Low-dimensional magnetic systems, those having magnetic interactions in only one or two dimensions, have become of increasing interest due to the enhanced importance of quantum fluctuations in these materials that lead to unique quantum behavior. A recent example is the molecular-based spin ladder bispiperdinium tetrabromocuprate [1] in which Luttinger liquid physics has been demonstrated for the first time [2]. This has been especially true of copper complexes due to the $S = ½$ nature of Cu(II). The key to the design and synthesis of such systems has been the use of appropriate ligands on Cu(II) to produce a viable magnetic superexchange pathway, while at the same time providing sufficient isolation between the structural motif components to allow the examination of the properties as a 1-D, or 2-D system over a reasonable range of temperature and applied field, before the onset of 3-D effects make the approximation

---

*Corresponding author. Email: Mturnbull@clarku.edu

ISSN 0095-8972 print/ISSN 1029-0389 online © 2011 Taylor & Francis
DOI: 10.1080/00958972.2010.543459

of a low-dimensional system invalid. To this end, pyrazine has been employed in the production of such systems. A number of 1-D and 2-D coordination polymers of Cu(II) have been prepared using pyrazine (pz) to provide both structural control, a result of its linear bridging mode, and a superexchange pathway with moderate exchange (~0 to −20 K) [3]. The moderate exchange value allows for detailed study in the ordered and disordered regimes *via* both variable temperatures and applied fields.

Dicyanoaurate [$Au(CN)_2^-$] also provides a potential tool for the construction of these low-dimensional lattices, specifically the one that can be used to control lattice dimensionality due to its near linearity and stability. It has been shown to provide a very poor superexchange pathway [4], and hence can be employed for the isolation of structural motifs although it has been reported to propagate weak ferromagnetic exchange in rare circumstances [5]. The moderate flexibility of the dicyanoaurate ion in its bridging mode, with M–Au–M angles ranging from 160° [6] to 180° [4a] and C≡N–M angles ranging from 144° [4a] to 177° [7], will accommodate a number of ancillary ligands on the metal ion while still maintaining a roughly linear geometry. In addition, gold–gold interactions may provide an additional structural component [4b, 4c, 8]. Such gold–gold interactions have a stabilizing effect similar to the strength of hydrogen bonding [6].

Previous studies have employed the pyrazine/dicyanoaurate ligand combination to prepare complexes of transition metal ions which showed 1-D, 2-D, and 3-D structural networks incorporating low-dimensional magnetic lattices [8c, 9]. We were specifically interested in the potential for preparing pyrazine-bridged, 2-D layers of Cu(II) ions linked, and therefore isolated, by the dicyanoaurate ions, essentially, the inverse of the previously reported complex $Cu(pz)[Au(CN)_2]_2$ [8c, 9]. In this case, however, the result was a unique 2-D structure with both coordinated and isolated dicyanoaurate ions. We report here the synthesis, structure, and magnetic properties of $[Cu(pz)(Au(CN)_2)(DMSO)_2]Au(CN)_2$ (**1**).

2. Experimental

All materials were purchased from Strem Chemical or Aldrich Chemical companies and used without purification. $Cu(pz)[Au(CN)_2]_2$ was prepared according to the literature [8c]. Infrared (IR) spectra were recorded as KBr pellets on a PE Spectrum 100. X-ray powder diffraction measurements were made on a Bruker AXS-D8 X-ray powder diffractometer. Thermal measurements were carried out on a Perkin Elmer Jade DSC from 30°C to 300°C at a heating rate of 10°C min^{-1}.

2.1. $[Cu(pz)(Au(CN)_2)(DMSO)_2]Au(CN)_2$ (1)

A solution of $Cu(ClO_4)_2$ (0.062 g, 0.17 mmol) in 1.5 mL of DMSO was added to a solution of pyrazine (0.0136 g, 0.17 mmol) in 1.0 mL of DMSO to produce a blue solution. To this a solution of $KAu(CN)_2$ (0.0979 g, 0.34 mmol) in 2.5 mL of DMSO was added dropwise with stirring. The pale teal solution was left open at room temperature for 4 days by which time green crystals had grown. The crystals were harvested through vacuum filtration to yield 0.075 g (57%) emerald green crystals.

Combustion analysis: Calcd for $C_{12}H_8N_6O_2S_2CuAu_2$ (%): C, 14.8; H, 1.10; N, 10.2; found (%): C, 14.6; H, 0.84; N, 10.3. IR (KBr) ν 3114 w, 2187 s, 2139 m, 1417 m, 1065 w, 1015 s, 945 m, 819 w, 490 m (cm^{-1}).

2.2. *Magnetic data*

Magnetic susceptibility data were collected using a Quantum Design MPMS-XL SQUID magnetometer. Isothermal magnetization at 1.8 K was collected in fields up to 5 T and several data points were collected as the field was reduced back to zero to check for hysteresis; none was observed. Temperature-dependent magnetization was collected in a field of 0.1 T from 1.8 to 310 K. Data were corrected for the sample holder, the temperature-independent paramagnetism of the Cu(II) ion and diamagnetic contributions of the constituent atoms [10].

2.3. *Single-crystal X-ray diffraction data*

X-ray data for **1** were collected with an Oxford Diffraction Gemini R CCD area detector using *CrysAlisPro* software and graphite-monochromated Mo-Kα ($\lambda = 0.71073$ Å) at 100(2) K. The structure was solved by direct methods using SHELXS97 [11] and expanded *via* Fourier techniques [12]. All non-hydrogen atoms were refined anisotropically by full-matrix least-squares on F^2 using SHELXL97. Hydrogens were placed in their calculated positions and refined *via* a riding model with fixed isotropic *U* values. An absorption correction was performed using *CrysAlisRED* and all calculations, including figures 1–3, were performed using SHELXTL [13]. Crystal and experimental data for **1** are listed in table 1. Scheme 1 for the molecular structure of **1** is shown. Bond lengths and angles are given in table 2. The structure of **1** has been deposited with the CCDC (Supplementary material). Comparison of X-ray powder diffraction data with the crystallographic data of **1** established that the samples used for magnetic studies were the same phase as the single crystal.

3. Results and discussion

3.1. *Synthesis and structure*

Reaction of copper perchlorate with potassium dicyanoaurate and pyrazine in DMSO gave $[Cu(pz)(Au(CN)_2)(DMSO)_2]Au(CN)_2$ (**1**) in 57% yield (scheme 1).

Single crystals suitable for X-ray diffraction were isolated directly from the reaction mixture. The compound crystallizes in the monoclinic space group *P2₁/c*. There are two distinct structural units in the crystal: the $[Cu(pz)(Au(CN)_2)(DMSO)_2]_n$ cation, containing Au1 (figure 1), and an uncoordinated $Au(CN)_2$ anion, containing Au2. Coordination about Au2 is linear as required by symmetry and the coordinated cyanides are nearly linear ($\angle_{Au2–C12–N12} = 178.0(4)°$). Au1 shows a similar structure, again linear at the Au ion as required by symmetry and $\angle_{Au1–C11–N11} = 179.8(3)°$. The C11–N11–Cu1 angle is slightly more distorted from linearity (176.6(2)°). The Cu1 is coordinated to two nitrogens from cyanide, two nitrogens from pyrazine rings, and two

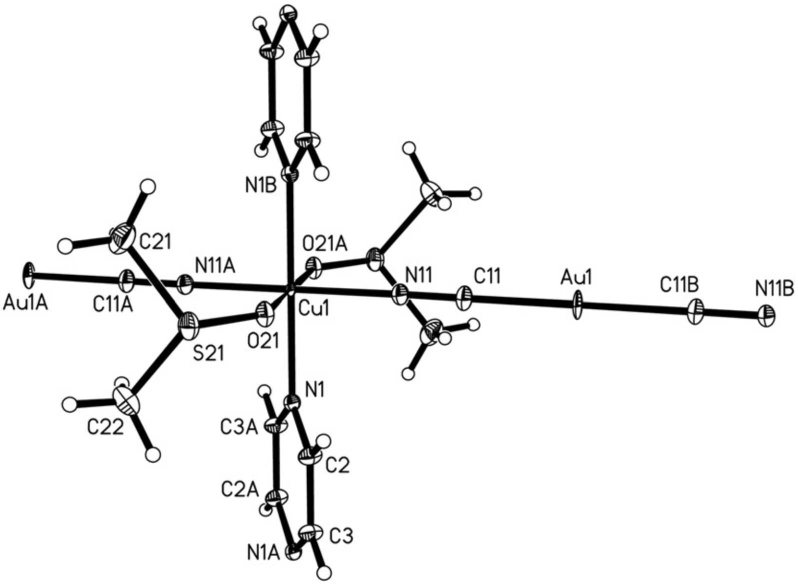

Figure 1. Thermal ellipsoid plot of **1** showing the coordination geometry about the metal ions. Hydrogens are shown as spheres of arbitrary size.

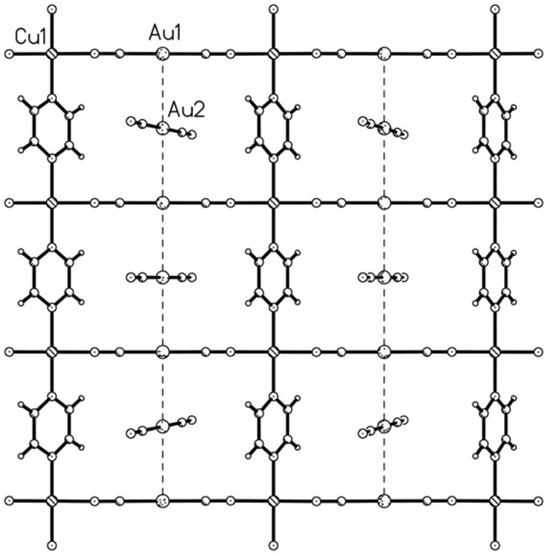

Figure 2. The layer structure of **1** viewed perpendicular to the C-face (*b*-horizontal, *a*-vertical).

oxygens from DMSO. It shows a typical Jahn–Teller distorted coordination geometry with four short bonds (Cu1–N1 = 2.050(2) Å, Cu1–N11 = 1.983(2) Å) and two elongated bonds (Cu1–O21 = 2.332(2) Å) and sits on a crystallographic inversion center; as such, all *trans* angles are 180°. The N1–Cu1–N11 angle is 90.04(9)°. The DMSO

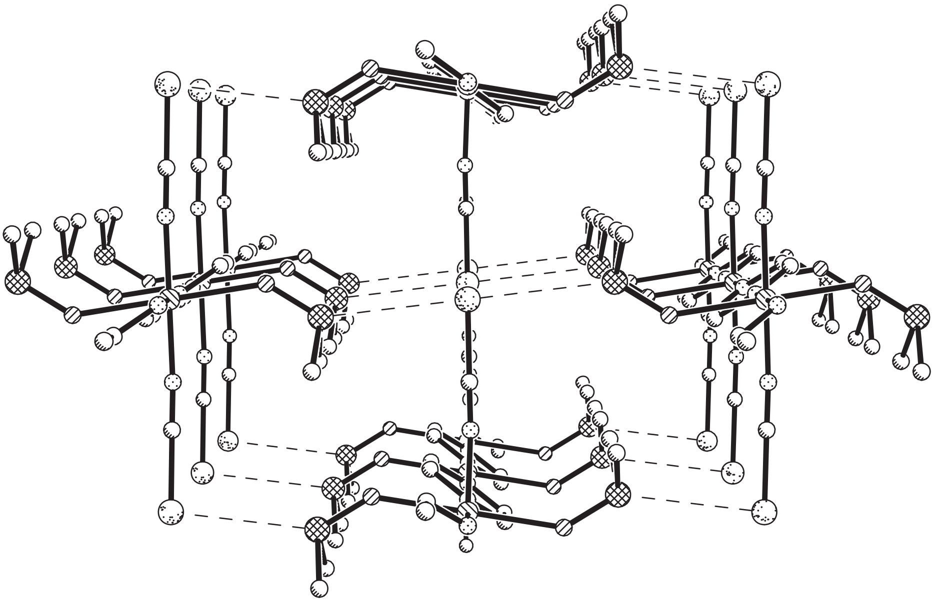

Figure 3. The crystal structure of **1** viewed parallel to the *a*-axis (*b*-axis vertical, *c*-axis horizontal) showing the contacts between DMSO sulfurs and Au1. Hydrogens have been removed for clarity.

Table 1. Crystal and experimental data for dicyanoaurate $[Au(CN)_2^-]$.

Empirical formula	$C_{12}H_4N_6O_2S_2Au_2Cu$
Formula weight	785.80
Temperature (K)	150(2)
Wavelength (Å)	0.71073
Crystal system	Monoclinic
Space group	$P2_1/c$
Unit cell dimensions (Å, °)	
a	6.8727(2)
b	10.2230(3)
c	14.1923(4)
α	90
β	90.0100(10)
γ	90
Volume (Å^3), Z	997.15(5), 2
Calculated density (Mg m^{-3})	2.617
Absorption coefficient (mm^{-1})	15.959
$F(000)$	706
Crystal size (mm^3)	$0.42 \times 0.26 \times 0.13$
θ range for data collection	2.46–36.34
Limiting indices	$-11 \leq h \leq 11$; $-16 \leq k \leq 16$; $-23 \leq l \leq 23$
Reflections collected	28,409
Independent reflection	4778 [R(int) = 0.0359]
Completeness to $\theta = 36.34$ (%)	98.5
Max. and min. transmission	0.2308 and 0.0571
Refinement method	Full-matrix least-squares on F^2
Data/restraints/parameters	4778/0/118
Goodness-of-fit on F^2	1.177
Final R indices [$I > 2\sigma(I)$]	$R_1 = 0.0263$, $wR_2 = 0.0803$
R indices (all data)	$R_1 = 0.0375$, $wR_2 = 0.0861$
Largest difference peak and hole (e Å^{-3})	2.627 and −3.281

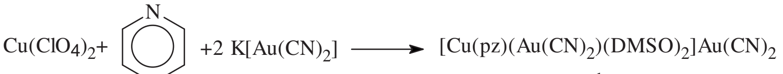
$Cu(ClO_4)_2$ + pyrazine + 2 $K[Au(CN)_2]$ → $[Cu(pz)(Au(CN)_2)(DMSO)_2]Au(CN)_2$

1

Scheme 1. Synthesis of **1**.

Table 2. Bond lengths [Å] and angles [°] for **1**.

Au(1)–C(11)#1	1.979(3)	Au(1)–C(11)	1.979(3)
Au(2)–C(12)	1.991(4)	Au(2)–C(12)#2	1.991(4)
Cu(1)–N(11)	1.983(3)	Cu(1)–N(11)#3	1.983(3)
Cu(1)–N(1)	2.050(2)	Cu(1)–N(1)#3	2.050(2)
Cu(1)–O(21)#3	2.332(2)	Cu(1)–O(21)	2.332(2)
S(21)–O(21)	1.523(2)	S(21)–C(21)	1.793(4)
S(21)–C(22)	1.793(4)	N(1)–C(2)	1.339(4)
N(1)–C(3)#4	1.340(4)	N(11)–C(11)	1.151(4)
C(3)–N(1)#4	1.340(4)	C(3)–C(2)	1.388(4)
N(12)–C(12)	1.144(5)	–	–
C(11)#1–Au(1)–C(11)	180.000(4)	C(12)–Au(2)–C(12)#2	180.0(3)
N(11)–Cu(1)–N(11)#3	180.0	N(11)–Cu(1)–N(1)	90.05(10)
N(11)#3–Cu(1)–N(1)	89.95(10)	N(11)–Cu(1)–N(1)#3	89.95(10)
N(11)#3–Cu(1)–N(1)#3	90.05(10)	N(1)–Cu(1)–N(1)#3	180.00(14)
N(11)–Cu(1)–O(21)#3	97.34(9)	N(11)#3–Cu(1)–O(21)#3	82.66(9)
N(1)–Cu(1)–O(21)#3	90.01(9)	N(1)#3–Cu(1)–O(21)#3	89.99(9)
N(11)–Cu(1)–O(21)	82.66(9)	N(11)#3–Cu(1)–O(21)	97.34(9)
N(1)–Cu(1)–O(21)	89.99(9)	N(1)#3–Cu(1)–O(21)	90.01(9)
O(21)#3–Cu(1)–O(21)	180.000(17)	O(21)–S(21)–C(21)	106.63(17)
O(21)–S(21)–C(22)	106.59(17)	C(21)–S(21)–C(22)	96.8(2)
C(2)–N(1)–C(3)#4	117.8(2)	C(2)–N(1)–Cu(1)	121.03(19)
C(3)#4–N(1)–Cu(1)	121.16(19)	C(11)–N(11)–Cu(1)	176.8(2)
N(11)–C(11)–Au(1)	179.9(3)	S(21)–O(21)–Cu(1)	138.99(15)
N(1)#4–C(3)–C(2)	121.2(3)	N(1)–C(2)–C(3)	121.0(3)
N(12)–C(12)–Au(2)	177.9(4)	–	–

Symmetry transformations used to generate equivalent atoms: #1 $-x+1, -y+2, -z$; #2 $-x, -y, -z$; #3 $-x+1, -y+1, -z$; #4 $-x+2, -y+1, -z$.

oxygen, O21, lies 89.99(8)° from N1, but is canted significantly relative to N11 ($\angle_{\mathrm{O21\text{–}Cu1\text{–}N11}} = 82.75(9)^{\circ}$). The bond angles within the pyrazine and DMSO molecules are unremarkable.

Pyrazines bridge Cu1 ions parallel to the *a*-axis while dicyanoaurate ions (Au1) bridge the Cu1 ions parallel to the *b*-axis producing polymeric rectangular sheets parallel to the C-face of the crystal. The Au2-containing dicyanoaurates fill the spaces in the rectangles and are held in place *via* gold–gold interactions (Au1–Au2 = 3.436(4) Å). Although Au–Au distances in the range 3.13–3.23 Å have been reported [8b, 14], longer interactions (as great as 3.6 Å) have also been noted [5, 6, 15]. The Au2(CN)$_2$ ions are inclined 22.7° relative to the normal to the layer. A final stabilizing structural motif is observed which links the layers into a 3-D network. There are short contacts between the sulfurs of DMSO and Au1 (S21–Au1 = 3.525(4) Å) (figure 3). Such short contacts have been observed previously between gold(I) ions and DMSO at slightly longer distances ranging from 3.551 Å [16] to 3.848 Å [17].

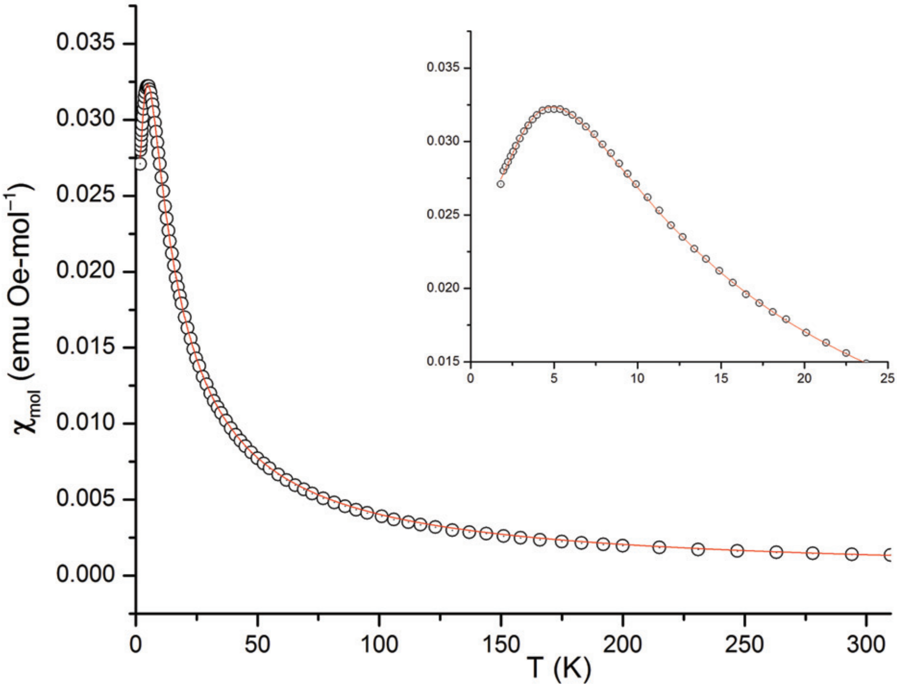

Figure 4. Magnetic susceptibility as a function of temperature for **1** from 1.8 to 310 K. The red line shows the fit to the 1-D Heisenberg model. The inset shows the expansion from 1.8 to 25 K and demonstrates the goodness-of-fit near the maximum.

3.2. *Magnetic behavior*

Magnetic susceptibility data were collected for **1** from 1.8 to 310 K and are presented in figure 4. The data exhibit a rounded maximum at 0.0325 emu Oe-mol^{-1} near 5 K, indicative of antiferromagnetic interactions and a low-dimensional magnetic lattice. The data were fit to the 1-D Heisenberg chain model [18] yielding $C = 0.421(1)$ emu-K Oe-mol^{-1}, $2J/k_B = -7.66(2)$ K and a paramagnetic impurity of 0.11(4)%. Attempts to fit the data to a 1-D Heisenberg chain model with a Curie–Weiss correction for interchain interactions gave values that were the same within experimental error and a Weiss constant of approximately zero (−0.02(1) K), indicating that the interchain interactions are negligible.

3.3. *Vapochromic behavior*

Compound **1** is stable in dry air. DSC measurements in dry N_2 show a sharp endotherm at 124.9°C (melting), followed by a broader endotherm from ~127°C to 150°C which we presume to be loss of DMSO. However, in the presence of significant humidity, the crystals lose DMSO, visibly changing from emerald green to light blue, and converts to the previously reported 3-D-coordination polymer [Cu(pz)(Au(CN)$_2$)$_2$] (**2**) as verified by IR and powder X-ray diffraction [8c, 9]. The conversion can be conveniently monitored by IR spectroscopy. Compound **1** shows two cyanide stretching bands at 2187 and 2139 cm^{-1}. After a period of 30 min to several hours (humidity dependent)

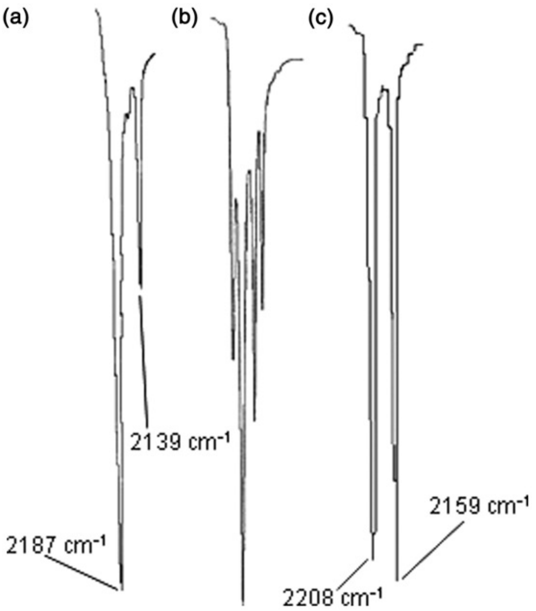

Figure 5. IR spectra showing the conversion of compound **1** to the desolvated compound **2**. (a) Fresh crystals of **1**; (b) crystals after approximately 1 h in humid air; (c) crystals of **1** after several hours in humid air showing conversion to **2**.

the complex has notably changed color and the IR spectrum shows four bands in the cyanide stretching region at 2208, 2187, 2159, and 2139 cm^{-1}. After several hours, the conversion is complete and once again, only two cyanide stretching vibrations are visible (2208 and 2159 cm^{-1}) (figure 5). Water appears to be necessary for the loss of DMSO from the complex, although it does not appear to be incorporated into the final product. A freshly prepared sample of **1** was divided and a portion was placed overnight in a desiccator while the other part of the sample was left on the bench. An IR spectrum of the sample in the desiccator showed no change from the spectrum of **1**, while the IR spectrum of the sample left on the bench (now blue) matched compound **2** by comparison of IR and powder X-ray diffraction pattern with an independently prepared sample of **2**. The process is reversible. A sample of **1** that had converted to **2** by exposure to air was placed in a sealed vial with a small cotton plug containing DMSO. After 24–48 h, the sample regained its green color and was shown to be compound **1** (with a small percentage of **2** remaining) by IR.

This behavior is not limited to gain and loss of DMSO. Samples of **1** or **2** (prepared by the loss of DMSO from **1**) provide a panoply of color when placed in sealed vials saturated with the vapors of a range of solvents. Not surprisingly, the time required for the change is directly related to the vapor pressure of the solvent. The reaction can be conveniently monitored by the changes in the C≡N stretching frequency in the IR. With ammonia, the change to a distinct purple occurs in a matter of minutes ($\nu_{C\equiv N} = 2172$, 2146 cm^{-1}). Other solvent vapors tested include propylamine (deep indigo blue, $\nu_{C\equiv N} = 2177$, 2166 cm^{-1}), pyridine (teal, $\nu_{C\equiv N} = 2216$, 2170 cm^{-1}), *N*-methylimidazole (dark purple, $\nu_{C\equiv N} = 2143$ cm^{-1}), and TMSO (bright green, $\nu_{C\equiv N} = 2214$, 2168 cm^{-1}). Conversion is faster starting with **2** prepared by the loss of DMSO from **1**.

4. Discussion

The interconversion of **1** and **2** appears to be catalyzed by moisture. Compound **1** is stable indefinitely at room temperature when stored in a desiccator or a sealed vial purged with dry N_2, as confirmed by DSC data which show no decomposition below the melting point (~125°C). However, the complex decomposes on the bench at room temperature at varying rates dependent upon humidity. This is further supported by the observation that the IR of the intermediate sample (figure 5b) also shows a significantly increased peak for water at both 3435 and 1635 cm^{-1}. Compound **1** clearly does not behave as a stable porous lattice given the substantial reorganization that is required for conversion to **2**. It appears to be a solid-state transformation, but single crystals of **1** do not retain their integrity.

The observation of an apparent water-catalyzed loss of DMSO is supported by the report by Leznoff *et al.* [14c] of similar behavior in $[\mathrm{Cu(Au(CN)_2)_2(DMSO)_2}]$. $[\mathrm{Cu(Au(CN)_2)_2(DMSO)_2}]$ exists as two polymorphs, both of which are thermally stable to at least 100°C, but both can be converted to $[\mathrm{Cu(Au(CN)_2)_2(H_2O)_2}]_n$ on standing in air. The process is reversible when a sample is placed in a DMSO atmosphere, although only one polymorph of $[\mathrm{Cu(Au(CN)_2)_2(DMSO)_2}]$ is obtained regardless of which form was used as the starting material. It appears that **1** shows similar reactivity. This suggests a process where the DMSO is displaced by H_2O to generate an aqua-adduct (whether lattice water or coordinated water is not known). The aqua adduct is not stable under ambient conditions and the water is subsequently lost, as evidenced by the isolation of the anhydrous **2**. The process is similar to that of nucleophilic catalysis in organic synthesis where an attacking nucleophile subsequently becomes a leaving group in the same reaction [19]. The DMSO molecules in **1** are coordinated much less strongly than those in $[\mathrm{Cu(Au(CN)_2)_2(DMSO)_2}]$ ($\mathrm{Cu–O} = 2.33$ Å in **1** *vs.* 1.95–2.02 Å). It may be the case that the other solvent adducts are similarly less tightly bound and, at least in the case of water, may be lost in the absence of the vapor.

Magnetic data show that **1** behaves as a well-isolated linear Heisenberg chain with an exchange constant in the typical range for pyrazine [3]. Although there have been some previous reports suggesting weak magnetic interactions supported by the dicyanoaurate ion [5] that does not appear to be the case here. Thus, it appears that **1** serves as another example of a mixed copper(II)/dicyanoaurate complex with distinct solvochromic behavior and which may also serve as a good example of a well-isolated linear Heisenberg chain. Experiments are in progress to isolate and characterize the various solvent adducts and determine the effect of changing solvents on the magnetic isolation of the Cu–pz chains.

Supplementary material

CCDC 785428 contains the supplementary crystallographic data for this article (compound **1**). These data can be obtained free of charge from The Cambridge Crystallographic Data Centre *via* www.ccdc.cam.ac.uk/data_request/.

Acknowledgments

The authors are grateful to Prof. Daniel B. Leznoff (Simon Fraser University) for many helpful suggestions.

References

[1] B.R. Patyal, B.L. Scott, R.D. Willett. *Phys. Rev. B*, **41**, 1657 (1990).

[2] M. Klanjsek, H. Mayaffre, C. Berthier, M. Horvatic, B. Chiari, O. Piovesana, P. Bouillot, C. Kollath, E. Orignac, R. Citro, T. Giamarchi. *Phys. Rev. Lett.*, **101**, 137201 (2008).

[3] (a) P.R. Hammar, M.B. Stone, D.H. Reich, C. Broholm, P.J. Gibson, M.M. Turnbull, C.P. Landee, M. Oshikawa. *Phys. Rev. B*, **59**, 1008 (1999); (b) B.R. Jones, P.A. Varughese, I. Olwjniczak, J.M. Pigos, J.L. Musfeldt, C.P. Landee, M.M. Turnbull, G.L. Carr. *Chem. Mater.*, **13**, 2127 (2001); (c) M.B. Stone, D.H. Reich, C. Broholm, K. Lefmann, C. Rischel, C.P. Landee, M.M. Turnbull. *Phys. Rev. Lett.*, **91**, 037205 (2003); (d) A.V. Sologubenko, K. Berggold, T. Lorenz, A. Rosch, E. Shimshoni, M.D. Phillips, M.M. Turnbull. *Phys. Rev. Lett.*, **98**, 107201 (2007); (e) F.M. Woodward, P.J. Gibson, G. Jameson, C.P. Landee, M.M. Turnbull, R.D. Willett. *Inorg. Chem.*, **46**, 4256 (2007); (f) F. Xiao, F.M. Woodward, C.P. Landee, M.M. Turnbull, C. Mielke, N. Harrison, T. Lancaster, S.J. Blundell, P.J. Baker, P. Babkevich, F.L. Pratt. *Phys. Rev. B*, **79**, 134412 (2009); (g) N. Tsyrulin, F. Xiao, A. Schneidewind, P. Link, H.M. Rønnow, J. Gavilano, C.P. Landee, M.M. Turnbull, M. Kenzelmann. *Phys. Rev. B*, **81**, 134409/1 (2010); (h) E. Cizmar, S.A. Zvyagin, R. Beyer, M. Uhlarz, M. Ozerov, Y. Skourski, J.L. Manson, J.A. Schlueter, J. Wosnitza. *Phys. Rev. B*, **81**, 064422/1 (2010); (i) J.L. Musfeldt, L.I. Vergara, T.V. Brinzari, C. Lee, L.C. Tung, J. Kang, Y.J. Wang, J.A. Schlueter, J.L. Manson, M.-H. Whangbo. *Phys. Rev. Lett.*, **103**, 157401/1 (2009); (j) J.L. Manson, J.A. Schlueter, K.A. Funk, H.I. Southerland, B. Twamley, T. Lancaster, S.J. Blundell, P.J. Baker, F.L. Pratt, J. Singleton, R.D. McDonald, P.A. Goddard, P. Sengupta, C.D. Batista, L. Ding, C. Lee, M.-H. Whangbo, I. Franke, S. Cox, C. Baines, D. Trial. *J. Am. Chem. Soc.*, **131**, 6733 (2009); (k) T. Lancaster, S.J. Blundell, M.L. Brooks, P.J. Baker, F.L. Pratt, J.L. Manson, M.M. Conner, F. Xiao, C.P. Landee, F.A. Chaves, S. Soriano, M.A. Novak, T.P. Papageorgiou, A.D. Bianchi, T. Herrmannsdorfer, J. Wosnitza, J.A. Schlueter. *Phys. Rev. B*, **75**, 094421/1 (2007); (l) J.L. Manson, T. Lancaster, J.A. Schlueter, S.J. Blundell, M.L. Brooks, F.L. Pratt, C.L. Nygren, H.-J. Koo, D. Dai, M.-H. Whangbo. *Inorg. Chem.*, **46**, 213 (2007); (m) W.E. Hatfield, J.F. Villa. *J. Am. Chem. Soc.*, **93**, 4081 (1971); (n) D.B. Losee, H.W. Richardson, W.E. Hatfield. *J. Chem. Phys.*, **59**, 3600 (1973); (o) H.W. Richardson, W.E. Hatfield. *J. Am. Chem. Soc.*, **98**, 835 (1976).

[4] (a) M.-L. Liu, L.-Z. Zhang, X.-P. Sun, Z.-P. Ma, W. Gu, X. Liu. *J. Coord. Chem.*, **61**, 2266 (2008); (b) J. Suarez-Varela, H. Sakiyama, J. Cano, E. Colacio. *Dalton Trans.*, 249 (2007); (c) C. Paraschiv, M. Andruh, S. Ferlay, M.W. Hosseini, N. Kyritsakas, J.-M. Planeix, N. Stanica. *Dalton Trans.*, 1195 (2005).

[5] D.B. Leznoff, B.-Y. Xue, B.O. Patrick, V. Sanchez, R.C. Thompson. *Chem. Commun.*, 259 (2001).

[6] J. Lefebvre, D. Chartrand, D.B. Leznoff. *Polyhedron*, **26**, 2189 (2007).

[7] A. Galet, M.C. Munoz, V. Martinez, J.A. Real. *Chem. Commun.*, 2268 (2004).

[8] (a) A.M. Madalan, N. Avarvari, M. Andruh. *Cryst. Growth Des.*, **6**, 1671 (2006); (b) W. Han, L. Yi, Z.-Q. Liu, W. Gu, S.-P. Yan, P. Cheng, D.-Z. Liao, Z.-H. Jiang. *Eur. J. Inorg. Chem.*, 2130 (2004); (c) D.B. Leznoff, B.-Y. Xue, C.L. Stevens, A. Storr, R.C. Thompson, B.O. Patrick. *Polyhedron*, **20**, 1247 (2001).

[9] W.-F. Yeung, W.-T. Wong, J.-L. Zuo, T.-C. Lau. *J. Chem. Soc., Dalton Trans.*, 629 (2000).

[10] R.L. Carlin. *Magnetochemistry*, Springer-Verlag, Berlin (1986).

[11] G.M. Sheldrick. *SHELXS97*, University of Göttingen, Göttingen, Germany (1997).

[12] G.M. Sheldrick. *SHELX97-2, Programs for the Solution and Refinement of Crystal Structures*, University of Göttingen, Göttingen, Germany (1997).

[13] Bruker. *SHELXTL*, Bruker AXS Inc., Madison (2006).

[14] (a) J. Qu, W. Gu, X. Liu. *J. Coord. Chem.*, **61**, 618 (2008); (b) J. Suarez-Varela, A.J. Mota, H. Aouryaghal, J. Cano, A. Rodriguez-Dieguez, D. Luneau, E. Colacio. *Inorg. Chem.*, **47**, 8143 (2008); (c) J. Lefebvre, R.J. Batchelor, D.B. Leznoff. *J. Am. Chem. Soc.*, **126**, 16117 (2004).

[15] I.K. Chu, I.P.Y. Shek, K.W.M. Siu, W.-T. Wong, J.-L. Zuo, T.-C. Lau. *New J. Chem.*, **24**, 765 (2000).

[16] D. Fernandez, M.I. Garcia-Seijo, M. Bardaji, A. Laguna, M.E. Garcia-Fernandez. *Dalton Trans.*, 2633 (2008).
[17] T.R. Smyth, B.R. Vincent, E.R.T. Tiekink. *CrystEngComm*, **2**, 115 (2000).
[18] D.C. Johnston, R.K. Kremer, M. Troyer, X. Wang, A. Klumper, S.L. Bud'ko, A.K. Panchula, P.C. Canfield. *Phys. Rev. B*, **61**, 9558 (2000).
[19] E.M. Cherkasova, S.V. Bogatkov, Z.P. Golovina. *Russ. Chem. Rev.*, **46**, 246 (1977).